Dalton Transactions

PAPER

View Article Online
View Journal | View Issue

Cite this: *Dalton Trans.*, 2018, **47**, 1117

Received 16th November 2017,
Accepted 5th December 2017

DOI: 10.1039/c7dt04327a

rsc.li/dalton

Preparation and reactivity of iron complexes bearing anionic carbazole-based PNP-type pincer ligands toward catalytic nitrogen fixation†

Junichi Higuchi, Shogo Kuriyama, Aya Eizawa, Kazuya Arashiba, Kazunari Nakajima and Yoshiaki Nishibayashi *

Iron–chloride, –dinitrogen, and –methyl complexes bearing anionic carbazole-based PNP-type pincer ligands are designed, prepared and characterized by X-ray analysis. Some iron complexes are found to work as catalysts toward nitrogen fixation under mild reaction conditions.

Introduction

The development of catalytic transformations of nitrogen gas in the presence of transition metal–dinitrogen complexes as catalysts under mild reaction conditions is one of the most important subjects in chemistry.[1] Since the first discovery of the direct and catalytic conversion of dinitrogen into ammonia under ambient reaction conditions reported by Schrock and co-workers in 2003,[2] some successful examples have been achieved by using molybdenum[3]–, iron[4]–, and cobalt[5]–dinitrogen complexes as catalysts. In 2010, we reported the catalytic formation of ammonia from nitrogen gas under ambient reaction conditions using a dinitrogen-bridged dimolybdenum–dinitrogen complex bearing pyridine-based PNP-type pincer ligands as a catalyst.[6,7] Quite recently, we have found a novel nitrogen fixation system *via* a direct cleavage of the nitrogen–nitrogen triple bond of molecular dinitrogen using molybdenum–iodide complexes bearing a PNP-pincer ligand.[8]

Based on our previous study, we have recently found that an iron–dinitrogen complex bearing an anionic pyrrole-based PNP-type pincer ligand ([Fe(N$_2$)(pyr-PNP)] **1a**; pyr-PNP = 2,5-bis(di-*tert*-butylphosphinomethyl)pyrrolide) worked as an effective catalyst in the reaction of dinitrogen gas with KC_8 as a reductant and [H(OEt$_2$)$_2$][BAr$^F_4$] as a proton source in Et$_2$O at −78 °C for 1 h to give a mixture of ammonia and hydrazine (14.3 equiv. and 1.8 equiv. based on the catalyst, respectively; 17.9 equiv. of fixed N atoms based on the catalyst) (Scheme 1).[9] In this reaction system, we isolated and characterized the corresponding iron–dinitrogen complex bearing a β-protonated pyrrole moiety (**2a**) from a stoichiometric reaction of **1a** with 1 equiv. of [H(OEt$_2$)$_2$][BAr$^F_4$].[9] Unfortunately, **2a** has a lower catalytic activity toward nitrogen fixation than **1a**. This experimental result indicates that **2a** is considered to be one of the deactivated species in the catalytic reaction. Quite recently, we have found that an iron–dinitrogen complex bearing a dimethyl-substituted pyrrole-based PNP-type pincer ligand (**1b**) worked as a more effective catalyst than **1a** toward the catalytic transformation, a mixture of ammonia and hydrazine being produced (22.7 equiv. and 1.7 equiv. based on the catalyst, respectively; 26.1 equiv. of fixed N atoms based on the catalyst) (Scheme 1).[10] However, a substantial improvement has not yet been achieved in the modified reaction system.

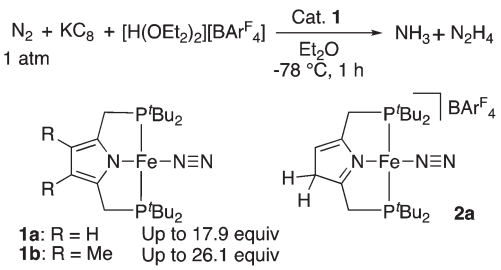

Scheme 1 Iron-catalysed reduction of dinitrogen using **1**.

Based on the previous findings, we have now newly designed and prepared novel iron–dinitrogen complexes bearing anionic carbazole-based PNP-type pincer ligands ([Fe(N$_2$)(carb-PNP)] **3**; carb-PNP = 1,8-bis(dialkylphosphinomethyl)-3,6-di-*tert*-butyl-carbazolide) because the protonation of the carbazole moiety may occur more hardly than that of the pyrrole moiety such as **1** (Chart 1). Herein, we report the preparation and reactivity of iron complexes bearing anionic carbazole-based PNP-type pincer ligands.

Department of Systems Innovation, School of Engineering, The University of Tokyo, Hongo, Bunkyo-ku, Tokyo 113-8656, Japan. E-mail: ynishiba@sys.t.u-tokyo.ac.jp

† Electronic supplementary information (ESI) available. CCDC 1546201, 1546204, 1546202 and 1546203. For ESI and crystallographic data in CIF or other electronic format see DOI: 10.1039/c7dt04327a

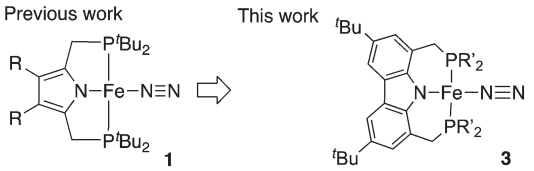

Chart 1 Iron–dinitrogen complex bearing a novel PNP-type pincer ligand.

Results and discussion

Gade and co-workers previously reported the preparation of carbazole-based PNP-type pincer ligands bearing Ph_2P, $^{i}Pr_2P$, and phospholane moieties.[11,12] According to their procedure,[11,12] 1,8-bis(bromomethyl)-3,6-di-*tert*-butyl-9*H*-carbazole (**4**) was prepared as a precursor of the corresponding PNP-type pincer ligands. The reaction of **4** with di-*tert*-butylphosphine and di-1-adamantylphosphine in acetone at reflux temperature gave 1,8-bis(di-*tert*-butylphosphinomethyl)-3,6-di-*tert*-butyl-9*H*-carbazole (**5a**) and 1,8-bis(di-1-adamantylphosphinomethyl)-3,6-di-*tert*-butyl-9*H*-carbazole (**5b**) in excellent yields, respectively (Scheme 2). The treatment of $[FeCl_2(thf)_{1.5}]$ with 1.0 equiv. of lithium carb-PNP, which were prepared from **5a** with 1.1 equiv. of ^{n}BuLi in THF at 0 °C for 1 h or generated *in situ* from **5b** with 1.1 equiv. of $LiN(SiMe_3)_2$ in THF at room temperature for 1 h, in toluene at room temperature afforded the corresponding iron–chloride complexes bearing the carb-PNP ligand [FeCl(carb-PNP)] (**6a** and **6b**) in 82% and 72% yields, respectively (Scheme 2). The molecular structures of **6a** and **6b** were confirmed by X-ray analysis.‡ The unit cell of **6a** contains two crystallographically independent molecules and one of them contains whole molecule disorder. The ORTEP drawings of **6a** and **6b** are shown in Fig. 1. The crystal structures of both **6a** and **6b** have distorted tetrahedral geometries around the iron atoms (the geometry index τ_4 = 0.79 for **6a** and 0.80 for **6b**, respectively), where τ_4 = 0.00 for a perfect square planar and τ_4 = 1.00 for a tetrahedral geometry.[13] Complexes **6a** and **6b** have solution magnetic moments of 4.9 ± 0.3μ_B and 4.7 ± 0.3μ_B at 298 K, respectively, which are consistent with the spin-only value for an S = 2 spin state (4.9μ_B).

Reduction of **6a** with 1.1 equiv. of KC_8 in THF at room temperature for 17 h under an atmospheric pressure of nitrogen gas gave a dinitrogen-bridged diiron complex bearing carb-PNP ligands $[Fe(carb\text{-}PNP)]_2(\mu\text{-}N_2)$ (**7a**) in 56% yield (Scheme 2). The molecular structure of **7a** was confirmed by X-ray analysis.‡ An ORTEP drawing of **7a** is shown in Fig. 2(a). The crystal structure of **7a** has a distorted tetrahedral geometry around the iron atom (τ_4 = 0.77 and 0.71 in two iron atoms, respectively) with a bridged dinitrogen ligand in an end-on fashion. The N–N bond length of 1.106(4) Å in **7a** indicates the weak activation of the coordinated dinitrogen. Similar dinitrogen-bridged diiron complexes with a tetrahedral geometry around the iron atoms have already been reported by other research groups.[14] Iron complex **7a** has a solution magnetic moment of 7.5 ± 0.7 at 298 K. When the magnetic moment and the tetrahedral structure are taken into consideration, complex **7a** can be assigned an S = 3 (6.9μ_B) state. No absorbance assignable to the terminal dinitrogen ligand in the IR spectra of a THF solution of **7a** or in a solid state (KBr) indi-

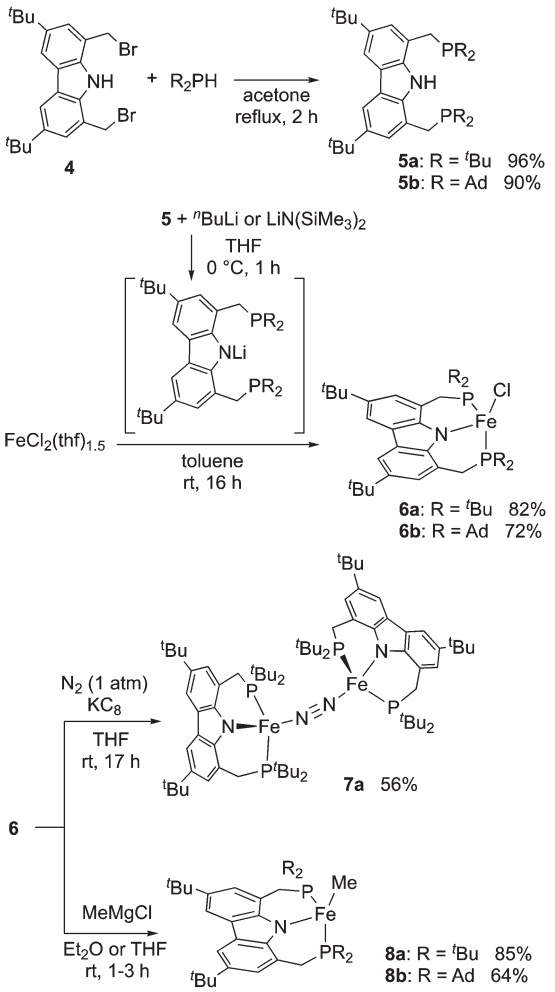

Scheme 2 Preparation of iron–dinitrogen and –methyl complexes.

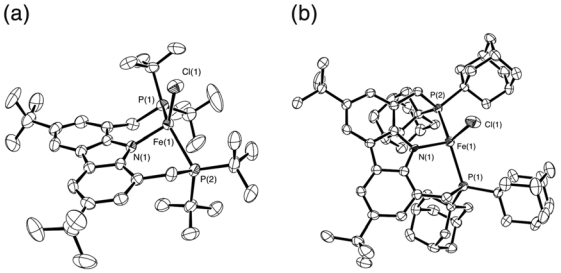

Fig. 1 ORTEP drawings of **6a** (a) and **6b** (b). Thermal ellipsoids are shown at the 50% level. Hydrogen atoms are omitted for clarity.

‡Crystal structures of **6a**, **6b**, **7a**, and **8a** were determined by X-ray analysis. See the ESI† for details.

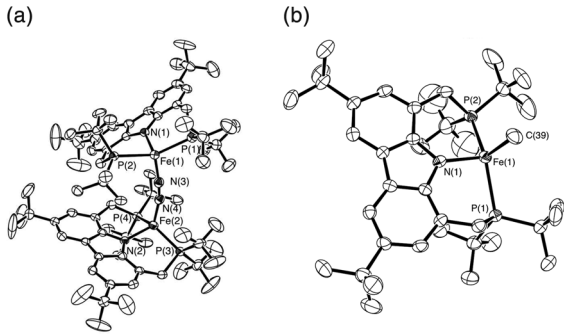

Fig. 2 ORTEP drawings of **7a** (a) and **8a** (b). Thermal ellipsoids are shown at the 50% level. Hydrogen atoms are omitted for clarity.

cates that the dinuclear structure remains in a THF solution of **7a**. Unfortunately, we cannot isolate the corresponding dinitrogen complex after the reduction of **6b** with KC_8 under an atmospheric pressure of nitrogen gas, where only an unidentified mixture was obtained.

Reactions of **6a** and **6b** with 1.1 equiv. of MeMgCl in Et_2O and THF at room temperature for 1–3 h afforded the corresponding methyl complexes [FeMe(carb-PNP)] (**8a** and **8b**) in 85% and 64% yields, respectively (Scheme 2). The molecular structure of **8a** was confirmed by X-ray analysis.‡ An ORTEP drawing of **8a** is shown in Fig. 2(b). The crystal structure of **8a** has a distorted tetrahedral geometry around the iron atom with τ_4 of 0.81. Iron complexes **8a** and **8b** have the same solution magnetic moment of 4.7 ± 0.3μ_B at 296 K. In both complexes, the spin state can be assigned $S = 2$ (4.9μ_B).

In sharp contrast to an intermediate spin square planar state of iron(II) complexes bearing a pyr-PNP pincer ligand,[9] the iron(II) complexes bearing a carb-PNP pincer ligand adopted a high spin tetrahedral geometry around the iron atom. We consider that the size of the chelate ring rather than the nature of the N-donor of the PNP-type pincer ligands determines the configuration of the iron complexes. As a result, the rigid nature of the pyr-PNP pincer ligand may favour the square planar geometry around the iron atom. On the other hand, the carb-PNP pincer ligand, which has two more methylene groups in the chelate ring, is considered to adopt a tetrahedral structure around the iron atom to decrease the strain of the chelate ring.

As shown in the previous sections, molecular structures are quite different between iron–dinitrogen complexes bearing pyr- and carb-PNP-type pincer ligands. While **1a** with a low spin square planar state adopted a mononuclear structure,[9] **7a** with a high spin tetrahedral state has been found to have a dinitrogen-bridged dinuclear structure in solid and solution states. These results indicate that the geometry around the iron atom determines the formation of a mononuclear or a dinuclear structure in the present system. At present, we consider that the tetrahedral configuration of **7a** decreases the steric hindrance around the coordinated dinitrogen to form a dinitrogen-bridged dinuclear structure.

Next, we investigated the catalytic reaction in the same experimental procedure[9] originally reported by Peters and coworkers.[4] The reaction of atmospheric dinitrogen gas with 40 equiv. of KC_8 as a reductant and 38 equiv. of $[H(OEt_2)_2][BAr^F{}_4]$ as a proton source in the presence of a catalytic amount of **7a** in Et_2O at −78 °C for 1 h gave only 0.5 equiv. of ammonia based on the iron atom of the catalyst together with 1.6 equiv. of hydrogen gas (Table 1, entry 1). No formation of ammonia was observed when THF was used as a solvent in place of Et_2O under the same reaction conditions, where only hydrogen (2.8 equiv. based on the iron atom of the catalyst) gas was observed (Table 1, entry 2). The use of methyl complex **8a** as a catalyst gave 1.9 equiv. of ammonia and 3.2 equiv. of hydrogen gas based on the iron atom, respectively (Table 1, entry 3). Interestingly, methyl complex bearing adamantyl groups at the phosphorus atom **8b** has a catalytic activity, where 3.2 equiv. of ammonia and 2.1 equiv. of hydrogen gas were produced based on the iron atom, respectively (Table 1, entry 4). When larger amounts of KC_8 and $[H(OEt_2)_2][BAr^F{}_4]$ were used, respectively, as a reductant and as a proton source, a mixture of ammonia and hydrazine (3.2 equiv. and 0.8 equiv. based on the iron atom, respectively) was obtained together with 3.4 equiv. of hydrogen gas (Table 1, entry 5). When **8** were used as pre-catalysts, the corresponding anionic mononuclear iron(0)–dinitrogen complexes such as **9** may be formed under catalytic reaction conditions (Scheme 3).

As shown in the previous section, the newly prepared dinuclear dinitrogen-bridged iron complex **7a** has no catalytic activity under the same reaction conditions. On the other hand, mononuclear methyl complexes **8** have a higher activity toward nitrogen fixation than **7a**, where **8b** with bulkier substi-

Table 1 Iron-catalyzed reduction of dinitrogen to ammonia and hydrazine[a]

$$\underset{1\ \text{atm}}{N_2} + KC_8 + [H(OEt_2)_2][BAr^F_4] \xrightarrow[Et_2O,\ -78\ ^\circ C,\ 1\ h]{\text{Catalyst}} NH_3 + N_2H_4$$

Entry	Catalyst	KC_8 (equiv.)[b]	$[H(OEt_2)_2][BAr^F{}_4]$ (equiv.)[b]	NH_3 (equiv.)[b]	N_2H_4 (equiv.)[b]	H_2 (equiv.)[b]
1	**7a**	40	38	0.5 ± 0.3[c]	<0.1[c]	1.6 ± 0.7[c]
2[d]	**7a**	40	38	<0.1	0	2.8
3	**8a**	40	38	1.9 ± 0.1[c]	0[c]	3.2 ± 0.2[c]
4	**8b**	40	38	3.2 ± 0.1[c]	0[c]	2.1 ± 0.3[c]
5	**8b**	80	76	3.2 ± 0.7[c]	0.8 ± 0.1[c]	3.4 ± 0.1[c]

[a] To a mixture of catalysts, KC_8 and $[H(OEt_2)_2][BAr^F{}_4]$ was added Et_2O at −78 °C, and then the resultant mixture was stirred at −78 °C for 1 h. [b] Equiv. based on the Fe atom. [c] An average of multiple runs (>2 times) is shown. [d] THF was used in place of Et_2O.

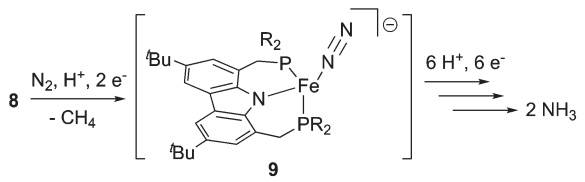

Scheme 3 Formation of anionic mononuclear iron–dinitrogen complex **9** from **8**.

tuents such as adamantyl groups at the phosphorus atom worked as a more effective catalyst than **8a**. These results indicate that the formation of anionic mononuclear iron(0)–dinitrogen complexes as key reactive intermediates of catalytic nitrogen fixation, which was proposed in the previous report by our group,[9] is more favoured from **8** than **7a**.

For a comparison of the catalytic activity of iron complexes bearing pyr- and carb-PNP-type pincer ligands, the molecular structure of the iron complexes is considered to be one of the most important factors toward catalytic nitrogen fixation. In fact, iron complexes bearing a pyr-PNP-type pincer ligand provide a square planar geometry around the iron atom. On the other hand, iron complexes bearing a carb-PNP-type pincer ligand provide a tetrahedral geometry around the iron atom. Although no direct relationship between the molecular structure and reactivity of iron complexes has yet been clarified in the present reaction system, we believe that the molecular structure of iron complexes has a great influence on the catalytic activity.

Conclusions

In summary, we have newly designed and prepared a series of anionic carbazole-based PNP-type pincer ligands. Iron–chloride, –methyl, and –dinitrogen complexes bearing these PNP-type pincer ligands have also been prepared and characterized by X-ray analysis. As a result, the iron–methyl complex bearing more bulkier substituents such as adamantyl groups at the phosphorus atom has been found to work as a catalyst toward nitrogen fixation under mild reaction conditions, where up to 4.8 equiv. of fixed N atoms were obtained as a mixture of ammonia and hydrazine. We believe that the experimental result described in this paper provides useful information to design more effective catalysts for nitrogen fixation.[15]

Conflicts of interest

The authors declare no competing financial interests.

Acknowledgements

The present project was supported by CREST, JST (JPMJCR1541). We are thankful for the Grants-in-Aid for Scientific Research (No. JP17H01201 and JP15H05798) from JSPS and MEXT. A. E. is a recipient of the JSPS Predoctoral Fellowships for Young Scientists. We also thank Dr Yoshiaki Tanabe of the University of Tokyo for his assistance in X-ray analysis.

Notes and references

1 For selected recent reviews, see: (*a*) K. C. MacLeod and P. L. Holland, *Nat. Chem.*, 2013, **5**, 559; (*b*) M. D. Fryzuk, *Chem. Commun.*, 2013, **49**, 4866; (*c*) H. Broda, S. Hinrichsen and F. Tuczek, *Coord. Chem. Rev.*, 2013, **257**, 587; (*d*) Y. Tanabe and Y. Nishibayashi, *Coord. Chem. Rev.*, 2013, **257**, 2551; (*e*) H.-P. Jia and E. A. Quadrelli, *Chem. Soc. Rev.*, 2014, **43**, 547; (*f*) C. J. M. van der Ham, M. T. M. Koper and D. G. H. Hetterscheid, *Chem. Soc. Rev.*, 2014, **43**, 5183; (*g*) C. Köthe and C. Limberg, *Z. Anorg. Allg. Chem.*, 2015, **641**, 18; (*h*) N. Khoenkhoen, B. de Bruin, J. N. H. Reek and W. I. Dzik, *Eur. J. Inorg. Chem.*, 2015, 567; (*i*) R. J. Burford and M. D. Fryzuk, *Nat. Rev. Chem.*, 2017, **1**, 0026; (*j*) Y. Roux, C. Duboc and M. Gennari, *ChemPhysChem*, 2017, **18**, 2606; (*k*) *Nitrogen Fixation; Topics in Organometallic Chemistry 60*, ed. Y. Nishibayashi, Springer, 2017.

2 (*a*) D. V. Yandulov and R. R. Schrock, *Science*, 2003, **301**, 76; (*b*) R. R. Schrock, *Angew. Chem., Int. Ed.*, 2008, **47**, 5512.

3 L. A. Wickramasinghe, T. Ogawa, R. R. Schrock and P. Müller, *J. Am. Chem. Soc.*, 2017, **139**, 9132.

4 (*a*) J. S. Anderson, J. Rittle and J. C. Peters, *Nature*, 2013, **501**, 84; (*b*) T. J. Del Castillo, N. B. Thompson and J. C. Peters, *J. Am. Chem. Soc.*, 2016, **138**, 5341; (*c*) P. J. Hill, L. R. Doyle, A. D. Crawford, W. K. Myers and A. E. Ashley, *J. Am. Chem. Soc.*, 2016, **138**, 13521; (*d*) M. J. Chalkley, T. J. Del Castillo, B. D. Matson, J. P. Roddy and J. C. Peters, *ACS Cent. Sci.*, 2017, **3**, 217; (*e*) T. M. Buscagan, P. H. Oyala and J. C. Peters, *Angew. Chem., Int. Ed.*, 2017, **56**, 6921.

5 S. Kuriyama, K. Arashiba, H. Tanaka, Y. Matsuo, K. Nakajima, K. Yoshizawa and Y. Nishibayashi, *Angew. Chem., Int. Ed.*, 2016, **55**, 14291.

6 (*a*) K. Arashiba, Y. Miyake and Y. Nishibayashi, *Nat. Chem.*, 2011, **3**, 120; (*b*) H. Tanaka, K. Arashiba, S. Kuriyama, A. Sasada, K. Nakajima, K. Yoshizawa and Y. Nishibayashi, *Nat. Commun.*, 2014, **5**, 3737; (*c*) S. Kuriyama, K. Arashiba, K. Nakajima, H. Tanaka, N. Kamaru, K. Yoshizawa and Y. Nishibayashi, *J. Am. Chem. Soc.*, 2014, **136**, 9719; (*d*) K. Arashiba, E. Kinoshita, S. Kuriyama, A. Eizawa, K. Nakajima, H. Tanaka, K. Yoshizawa and Y. Nishibayashi, *J. Am. Chem. Soc.*, 2015, **137**, 5666; (*e*) S. Kuriyama, K. Arashiba, K. Nakajima, H. Tanaka, K. Yoshizawa and Y. Nishibayashi, *Chem. Sci.*, 2015, **6**, 3940; (*f*) A. Eizawa, K. Arashiba, H. Tanaka, S. Kuriyama, Y. Matsuo, K. Nakajima, K. Yoshizawa and Y. Nishibayashi, *Nat. Commun.*, 2017, **8**, 14874.

7 (*a*) Y. Nishibayashi, *Inorg. Chem.*, 2015, **54**, 9234; (*b*) Y. Tanabe and Y. Nishibayashi, *Chem. Rec.*, 2016, **16**,

1549; (*c*) H. Tanaka, Y. Nishibayashi and K. Yoshizawa, *Acc. Chem. Res.*, 2016, **49**, 987.

8 K. Arashiba, A. Eizawa, H. Tanaka, K. Nakajima, Y. Yoshizawa and Y. Nishibayashi, *Bull. Chem. Soc. Jpn.*, 2017, **90**, 1111.

9 S. Kuriyama, K. Arashiba, K. Nakajima, Y. Matsuo, H. Tanaka, K. Ishii, K. Yoshizawa and Y. Nishibayashi, *Nat. Commun.*, 2016, **7**, 12181.

10 Y. Sekiguchi, S. Kuriyama, A. Eizawa, K. Arashiba, K. Nakajima and Y. Nishibayashi, *Chem. Commun.*, 2017, **53**, 12040.

11 (*a*) N. Grüger, L.-I. Rodríguez, H. Wadepohl and L. H. Gade, *Inorg. Chem.*, 2013, **52**, 2050; (*b*) G. T. Plundrich, H. Wadepohl and L. H. Gade, *Inorg. Chem.*, 2016, **55**, 353.

12 (*a*) V. C. Gibson, S. K. Spitzmesser, A. J. P. White and D. J. Williams, *Dalton Trans.*, 2003, 2718; (*b*) D. Bézier, C. Guan, K. Krogh-Jespersen, A. S. Goldman and M. Brookhart, *Chem. Sci.*, 2016, **7**, 2579.

13 L. Yang, D. R. Powell and R. P. Houser, *Dalton Trans.*, 2007, 955.

14 (*a*) T. A. Betley and J. C. Peters, *J. Am. Chem. Soc.*, 2004, **126**, 6252; (*b*) J. M. Smith, A. R. Sadique, T. R. Cundari, K. R. Rodgers, G. Lukat-Rodgers, R. J. Lachicotte, C. J. Flaschenriem, J. Vela and P. L. Holland, *J. Am. Chem. Soc.*, 2006, **128**, 756; (*c*) A. McSckimming and W. H. Harman, *J. Am. Chem. Soc.*, 2015, **137**, 8940; (*d*) T. Suzuki, Y. Wasada-Tsutsui, T. Ogawa, T. Inomata, T. Ozawa, Y. Sakai, M. D. Fryzuk and H. Masuda, *Inorg. Chem.*, 2015, **54**, 9271.

15 (*a*) S. Kuriyama, K. Arashiba, K. Nakajima, H. Tanaka, K. Yoshizawa and Y. Nishibayashi, *Eur. J. Inorg. Chem.*, 2016, 4856; (*b*) R. Imayoshi, K. Nakajima and Y. Nishibayashi, *Chem. Lett.*, 2017, **46**, 466; (*c*) R. Imayoshi, K. Nakajima, J. Takaya, N. Iwasawa and Y. Nishibayashi, *Eur. J. Inorg. Chem.*, 2017, 3769; (*d*) Y. Tanabe, K. Arashiba, K. Nakajima and Y. Nishibayashi, *Chem. – Asian J.*, 2017, **12**, 2544.